Fractal Aggregations at Low Driving Force with Strong Anisotropy

Mu Wang,[1] Xiao-Yong Liu,[1] Christina S. Strom,[2] Piet Bennema,[2] Willem van Enckevort,[2] and Nai-Ben Ming[1]
[1]*National Laboratory of Solid State Microstructures, Nanjing University, Nanjing 210093, China*
and Center for Advanced Studies of Science and Technology of Microstructures, Nanjing 210093, China
[2]*Laboratory of Solid State Chemistry, Faculty of Science, University of Nijmegen, 6525ED Nijmegen, The Netherlands*
(Received 16 September 1997)

In this Letter we report a unique fractal aggregation behavior of NH_4Cl crystallites grown in agarose gel. The fractal branches consist of faceted crystallites with remarkable correlations in their crystallographic orientations, which are formed by successive heterogeneous nucleations. Unlike the conventional fractal growth, this aggregation process occurs at a low growth driving force with strong crystallographic anisotropy, which leads to the ordering in the fractal branches. [S0031-9007(98)05675-0]

PACS numbers: 61.43.Hv, 47.53.+n, 64.60.Qb, 81.10.Aj

Fractal aggregation is one of the most intensively investigated topics in pattern formation studies [1–4]. In the past years the model known as diffusion-limited aggregation (DLA) [5–9] has been successfully introduced to different systems to interpret the ramified growth controlled by diffusive processes [10–13]. It is generally accepted that fractal aggregation occurs at situations far from thermodynamic equilibrium and where noise plays an important role. The anisotropy is usually very weak in the growth process, so tip splitting easily occurs. Besides, it has been reported for a number of systems that the fractals are polycrystalline or even in an amorphous state with a rough interfacial morphology [14–16]. It is generally believed that fractal aggregate is a random association of rough crystallites generated at high driving force. In this Letter, a novel type of fractal growth occurring at low driving force with strong anisotropy is presented. Optical and atomic force microscopies show that the fractal branches consist of faceted crystallites with remarkable correlations on their crystallographic orientations, which form a fairly strict periodic zigzag pattern.

The experiments were carried out in a thin layer of agarose gel containing NH_4Cl sandwiched by two cleaned glass plates. The thickness of the gel was about 100 μm for all runs. The gel was prepared by dissolving 130 mg agarose (Merck) into 50 ml of deionized, hot water. NH_4Cl (A.R. grade, 99.9%) was subsequently added, and the concentration was in the range of 2.5% to 5%. The glass cell was filled with the hot solution and a compact gel was formed after cooling down. A supersaturation was generated when the water in the gel medium gradually evaporated through the edges of the growth cell. The evaporation of water was not completely controlled in our experiment, yet it was a slow process comparing to the fractal aggregation, especially when a shell of NH_4Cl/agarose was formed at the edges of the cell. Therefore we expect that the driving force for the fractal growth remained relatively stable. The NH_4Cl crystallites usually nucleated on the glass plates by heterogeneous nucleation. The growth rate of the crystallites was about 2.0 μm/min in average, which is extremely slow comparing to usual NH_4Cl dendritic growth [16–18]. The fractal aggregates were observed *in situ* by a research optical microscope (Leitz, Orthoplan-pol). The morphology of the crystallites in the fractal branches was further studied by an atomic force microscope (AFM) (Digital Instruments, Nanoscope IIIa).

The typical fractal-like pattern observed in our system is shown in Fig. 1(a). The ramified branches originated from a central nucleus, which was formed by spontaneous nucleation, and grew radially outward. Compared to the fractals of DLA [5–9] and that of nucleation-limited aggregation (NLA) [19], this fractal pattern is more compact. Closer inspection shows that ordered structures exist in the fractal branches [cf. Figs. 1(b) and 1(c)]. The strongly correlated orientations of the crystallites lead to a zigzag pattern. In this case the fractal aggregation is not completely random. Many crystallites possess a shape reminiscent to a triangular pyramid, which in a few cases form closed loops, as indicated by the arrows in Figs. 1(b) and 1(c). This feature cannot be found in DLA, where the branches tend to avoid each other. *In situ* optical microscopy showed that the zigzag branches are generated by successive nucleation [20].

AFM indicates that two types of faceted crystallites can be identified in the fractal branches (Fig. 2). One possesses the shape of a triangular pyramid, sometimes truncated, with its threefold axis perpendicular to the substrate (type *A*). The other type is an elongated one, with two well defined facets on the top, and two side faces along the elongated direction (type *B*). Figure 2(a) indicates that *B* connects to one of the vertices of *A* in its elongated direction. Alternating nucleation of crystallites *A* and *B* forms the zigzagged branch. Figure 2(b) illustrates the connection of a crystallite of type *A* with three elongated crystallites of type *B*. Bunched steps can be observed on the side faces of the *B*-type crystallites, indicating that these faces are really faceted and they grew at a supersaturation lower than that for kinetic roughening.

From the crystallographic symmetry and the microscopic morphology of the faceted crystallites it is possible to estimate their crystallographic orientations. It

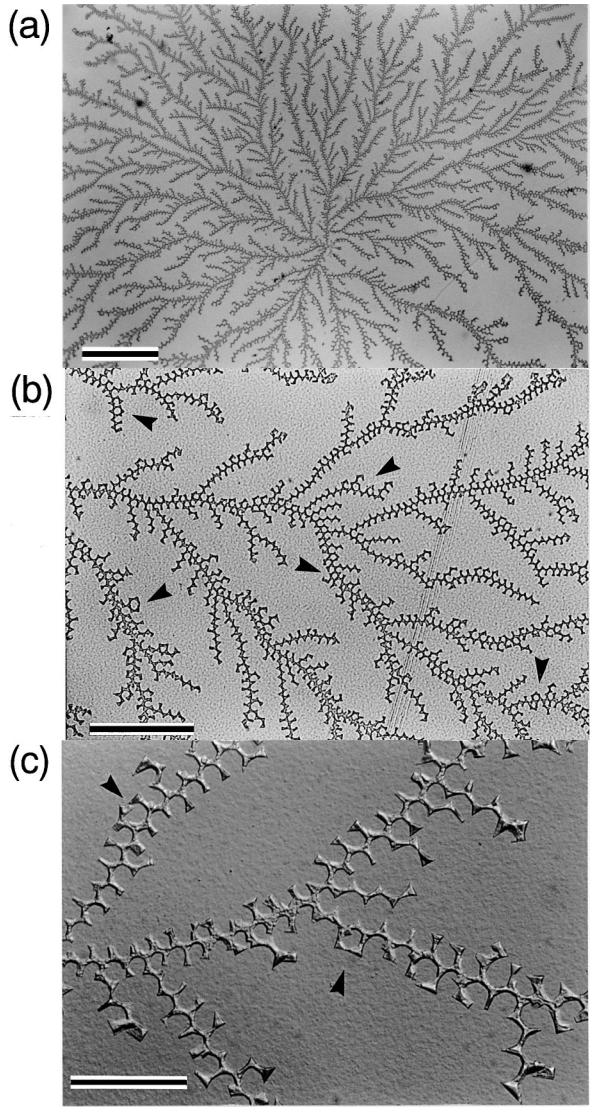

FIG. 1. (a) A fractal aggregate of NH_4Cl crystallites observed several millimeters away from the edge of the growth cell. The horizontal size of the cell is 18×18 mm^2. The branches of the fractal pattern are rather dense comparing to that of DLA. The bar represents 100 μm. (b) Higher magnification view of the zigzag fractal branches. The closed loops, usually hexagonal, are indicated by the arrows. The bar represents 50 μm. (c) The branches of the fractals observed by interference contrast microscopy. The orientation of the crystallites is closely correlated and many crystallites show the shape of a pyramid. The bar represents 25 μm.

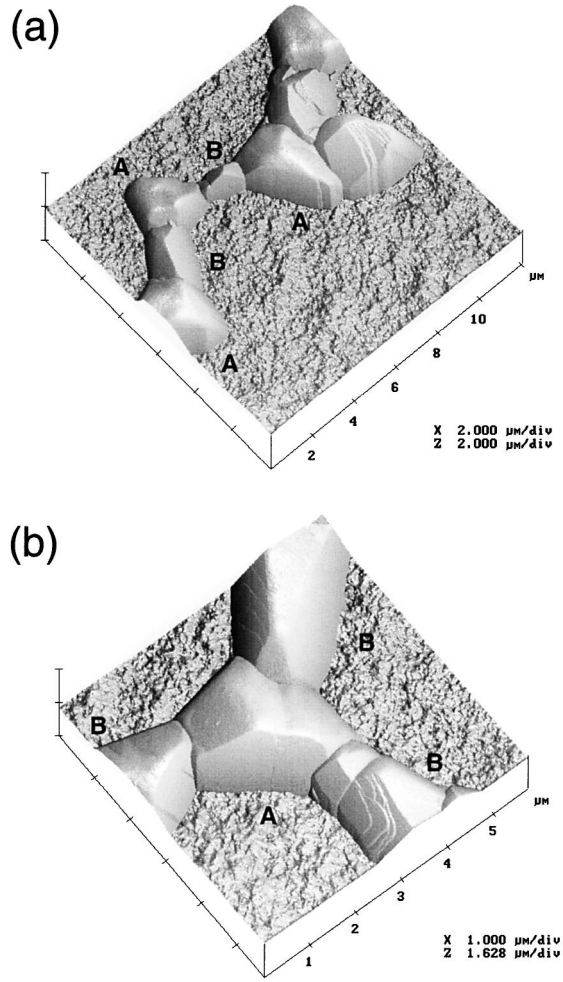

FIG. 2. (a) AFM micrograph of a zigzagged branch of the fractals. Two types of crystallite morphologies, denoted as *A* and *B*, respectively, appear alternatingly. (b) AFM micrograph of a junction area of a fractal branch. The threefold symmetry of the crystallite *A* is clear. On the side faces of crystallites *B*, macro steps can be clearly seen.

is known that the crystals of NH_4Cl possess the space group symmetry $Pm\bar{3}m$. NH_4^+ and Cl^- are located at $(0,0,0)$ and $(\frac{1}{2},\frac{1}{2},\frac{1}{2})$, respectively. The analysis based on the periodic bond chain (PBC) theory [21] with first nearest neighbor interactions shows that NH_4Cl has PBCs in directions $\langle 100\rangle$, $\langle 110\rangle$, and $\langle 111\rangle$ [22]. Combining these PBCs gives rise to the theoretically flat faces (F) of the forms $\{110\}$, $\{100\}$, and $\{111\}$. When a crystallite grows in a polar medium, such as water or gels containing aqueous solution, the nonpolar F faces $\{110\}$ seem to be suppressed [22]. Experimentally, a number of observations [16–18] indicated that the dendrites of NH_4Cl prefer to grow in $\langle 100\rangle$ directions. We expect that this feature is preserved in the growth of faceted crystallites. It follows that $\{100\}$ grows much faster than the others, and it is finally replaced by a group of four $\{211\}$ faces. Early precise studies of the morphology of NH_4Cl crystals grown from vapor and aqueous solutions showed that faces $\{211\}$ are indeed frequently observed [23]. In our experiments the shape of NH_4Cl crystallite is determined by $\{111\}$ and $\{211\}$ faces, as shown in Fig. 3(a).

Suppose a crystallite is initially oriented as that shown in Fig. 3(a). The glass substrate suppresses the development of the lower part of the octahedron. Note that the $\{211\}$ facets form a pyramid pointing along $\langle 100\rangle$, which is the fastest growth direction of NH_4Cl [16–18], and the $\{211\}$ faces develop faster than $\{111\}$. Consequently the crystallite is sharpened along $\langle 100\rangle$, and the supersaturation at the summit of the $\{211\}$ pyramids increases. Once the local supersaturation becomes higher than the nucleation barrier for heterogeneous nucleation, crystallite *B*

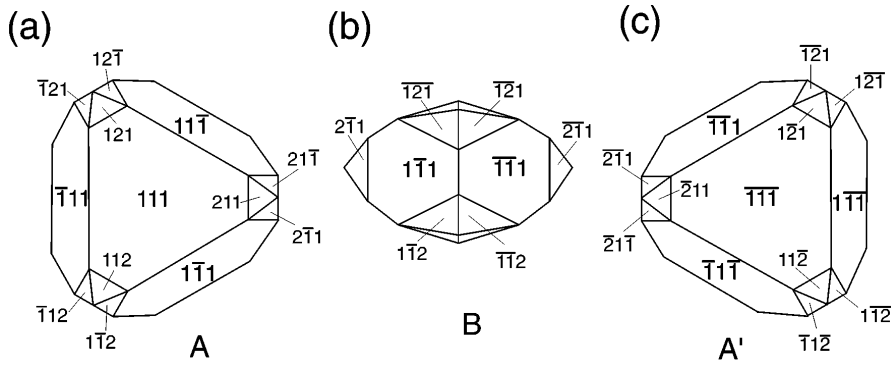

FIG. 3. The suggested morphologies of crystallites of A and B and the indexes of the faces based on PBC analysis.

nucleates. In our experimental conditions, the nucleus is energetically preferred to nucleate on one of the $\{211\}$ faces of A, say, $(2\bar{1}\,\bar{1})$. We suggest that the nucleus possesses the shape of truncated octahedron and the face that is in contact with A is also $[2\bar{1}\,\bar{1}]$. In addition, crystallite B is rotated for 78.5° along the $[2\bar{1}\,\bar{1}]$ direction of A [22]. The final orientation of B is shown in Fig. 3(b). Meanwhile the axis $[100]$ of B happens to point to the direction with higher supersaturation. Consequently, crystallite B grows faster along $[100]$ and is elongated. As the growth of the elongated B proceeds, a new nucleus will again be generated on its moving tip, where a group of four $\{211\}$ faces is located and feels the highest supersaturation. Suppose the nucleus is generated on $[\bar{2}\,\bar{1}\,\bar{1}]$ of B, and holds an octahedral shape. For this nucleus there are two equivalent $\langle 100\rangle$ directions, $[0\bar{1}0]$ and $[00\bar{1}]$, which orient to higher supersaturation. The simultaneous growth in these two directions helps to maintain the shape of pyramid. We denote this new nucleus as A', as shown in Fig. 3(c). It can be found easily that crystallites A and A' are inverse in orientations. When the fractal growth proceeds, new nuclei of type B will again be generated on the tips along $[0\bar{1}0]$ and $[00\bar{1}]$ directions. If nuclei emerge only on one of these two directions, the zigzag branch will be lengthened; if two nuclei are developed simultaneously on the two directions, then branching occurs. The above heterogeneous nucleation process repeats and finally generates a fractal pattern with zigzag branches.

To quantitatively characterize the fractal pattern shown in Fig. 1(a), we digitized it and calculated its spectrum of singularity $f(\alpha)$. With the method proposed by Argoul *et al.* [24], $f(\alpha)$ can be directly computed without resorting to an explicit Legendre transformation. The result is shown in Fig. 4(a). For comparison, we also computed $f(\alpha)$ of the NLA fractal pattern observed in the growth of $Ba(NO_3)_2$ [19] [Fig. 4(b)] and a computer-generated DLA cluster [Fig. 4(c)]. It is clear that none of these fractal patterns are globally self-similar. The maximum value of $f(\alpha)$, D_0, is different for the three fractals. For the pattern shown in Fig. 1(a), $D_0 = 1.82$, which is the most condensed one; for the NLA cluster of $Ba(NO_3)_2$, which was formed by random successive nucleation, $D_0 = 1.78$; for DLA, $D_0 = 1.67$, which is the lowest among the three fractals. The DLA is controlled by diffusion only, without surface kinetics and crystallographic preference in the aggregation process. So the screening effect is evident, and the overall pattern is rarified. The fractal pattern presented in this Letter, however, is determined by both nucleation process and crystallographic orientations of nuclei. As we reported before [19], the random-nucleation-controlled aggregate has higher fractal dimension than DLA. The influence of crystallographic anisotropy in nucleation process makes the fractal pattern even more compact. Figure 4 also shows that for the three clusters α takes on values in a finite range $[\alpha_{\min}, \alpha_{\max}]$. It is known that $\alpha_{\min} = \lim_{q\to\infty} D_q$ and $\alpha_{\max} = \lim_{q\to-\infty} D_q$ characterize the scaling properties of the most concentrated and most rarified regions of the fractal object, respectively. For the nucleation-controlled aggregation, regardless of the nucleation manner and the crystallographic details, the scaling properties at both limits $q \to \infty$ and $q \to -\infty$ are almost the same [cf. Figs. 4(a) and 4(b)]. DLA is more rarified in both the concentrated and the scanty distributed regions. Figure 4 implies that the nucleation-controlled growth is indeed different from the conventional diffusion-limited aggregation.

The fractal growth reported here shows some unique features, which provide in-depth insights into the fractal growth mechanism. In our case the NH_4Cl crystallites in the fractal branches are faceted, and they grow much slower than the kinetically roughened dendrites. This fact indicates that the driving force for the fractal growth is even lower than the critical supersaturation for kinetic roughening. Therefore it seems that the fractal growth does not arise exclusively in far-from-equilibrium situations; neither does the driving force for fractal aggregation need to be larger than that for dendritic growth. Another interesting feature is that the crystallographic orientation and the surface kinetics play an important role in the fractal aggregation. These ingredients, especially the crystallographic influence in the nucleation process, are not expected in the conventional fractal growth in Laplacian fields. In fact, anisotropy and surface kinetics

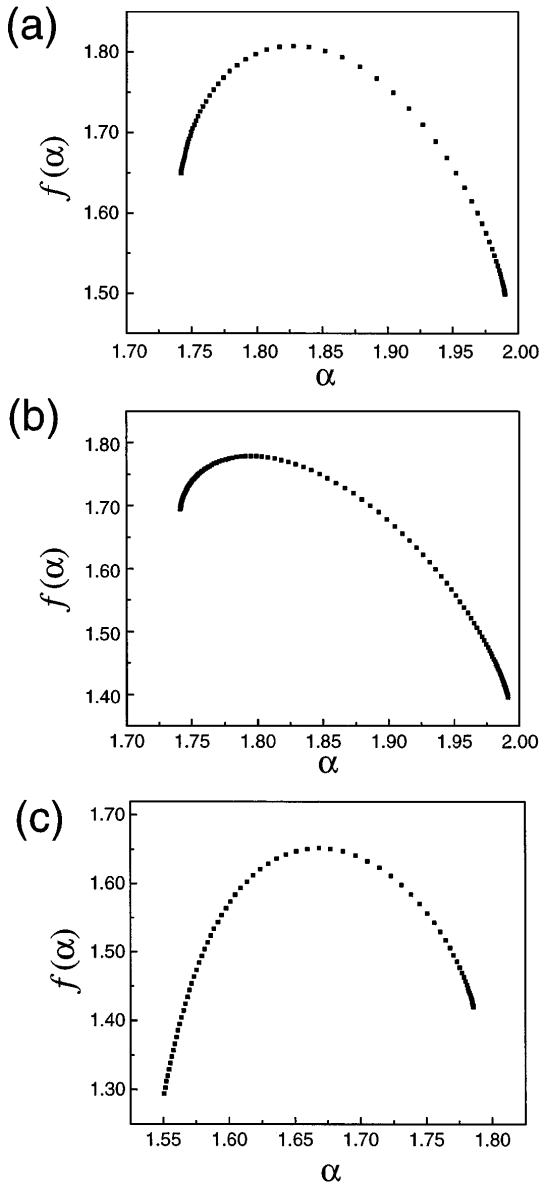

FIG. 4. (a) The singularity spectrum $f(\alpha)$ of the fractals of NH_4Cl shown in Fig. 1(a). $D_0 = 1.82$ in this case. (b) $f(\alpha)$ of the fractals of $Ba(NO_3)_2$ grown by random successive nucleation [19]. $D_0 = 1.78$. (c) $f(\alpha)$ of a computer-generated DLA. $D_0 = 1.67$.

normally stabilize the interfacial growth. In addition, it seems that the nucleation-controlled aggregation with strong crystallographic anisotropy is not a rarely occurring phenomenon. Similar zigzag aggregation behavior was observed in the crystallization of $FeSO_4$ from an aqueous solution film [20]. This aggregation behavior raises several challenging questions to the fractal growth mechanism, which deserve further studies.

The authors thank Dr. X-Y Liu and Dr. R. Grimbergen for discussions. This work was supported by the NSF of China (Project No. 19425007) and the Chinese Committee of Science and Technology. The support of the Qiu Shi Foundation of Science and Technology and the Netherlands Technology Foundation (STW) are also acknowledged.

[1] T. Vicsek, *Fractal Growth Phenomena* (World Scientific, Singapore, 1992), 2nd ed.
[2] J. S. Langer, Rev. Mod. Phys. **52**, 1 (1980).
[3] D. A. Kessler, J. Koplik, and H. Levine, Adv. Phys. **37**, 255 (1988).
[4] E. Ben Jacob and P. Garik, Nature (London) **343**, 523 (1990).
[5] T. A. Witten and L. M. Sander, Phys. Rev. Lett. **47**, 1400 (1981); Phys. Rev. B **27**, 5686 (1983).
[6] P. Meakin, Phys. Rev. A **27**, 1495 (1983).
[7] D. S. Graff and L. M. Sander, Phys. Rev. E **47**, R2273 (1993).
[8] H. Kaufman, A. Vespignani, B. B. Mandelbrot, and L. Woog, Phys. Rev. E **52**, 5602 (1995).
[9] T. C. Halsey, B. Duplantier, and K. Honda, Phys. Rev. Lett. **78**, 1719 (1997).
[10] R. Brady and R. C. Ball, Nature (London) **309**, 225 (1984).
[11] J. Nittmann, G. Daccord, and H. E. Stanley, Nature (London) **314**, 141 (1985).
[12] Mu Wang and Nai-ben Ming, Phys. Rev. A **45**, 2493 (1992); Phys. Rev. Lett. **71**, 113 (1993).
[13] Mu Wang, Nai-ben Ming, and P. Bennema, Phys. Rev. E **48**, 3825 (1993).
[14] C. H. Shang, Phys. Rev. B **53**, 13 759 (1996).
[15] G. Deutscher and Y. Lereah, Phys. Rev. Lett. **60**, 1510 (1988); Y. Lereah, G. Deutscher, and E. Grünbaum, Phys. Rev. A **44**, 8316 (1991).
[16] M. Yasui and M. Matsushita, J. Phys. Soc. Jpn. **61**, 2327 (1992).
[17] H. Honjo and S. Ohta, Phys. Rev. A **45**, R8332 (1992).
[18] A. Dougherty and R. Chen, Phys. Rev. A **46**, R4508 (1992).
[19] Nai-Ben Ming, Mu Wang, and Ru-Wen Peng, Phys. Rev. E **48**, 621 (1993).
[20] Mu Wang *et al.* (to be published).
[21] P. Bennema and J. P. van der Eerden, in *Morphology of Crystals*, edited by I. Sunagawa (Terra, Tokyo, 1987), pp. 1–75.
[22] C. S. Strom *et al.* (to be published).
[23] P. Groth, *Chemische Krystallographie* (Wilhelm Engelmann, Leipzig, 1906), pp. 182–184.
[24] F. Argoul, A. Arneodo, J. Elezgaray, G. Grasseau, and R. Murenzi, Phys. Rev. A **41**, 5537 (1990).